

# Ensemble Clustering via Co-association Matrix Self-enhancement

Yuheng Jia, *Member, IEEE*, Sirui Tao, Ran Wang, *Member, IEEE*, Yongheng Wang

**Abstract**—Ensemble clustering integrates a set of base clustering results to generate a stronger one. Existing methods usually rely on a co-association (CA) matrix that measures how many times two samples are grouped into the same cluster according to the base clusterings to achieve ensemble clustering. However, when the constructed CA matrix is of low quality, the performance will degrade. In this paper, we propose a simple yet effective CA matrix self-enhancement framework that can improve the CA matrix to achieve better clustering performance. Specifically, we first extract the high-confidence (HC) information from the base clusterings to form a sparse HC matrix. By propagating the highly-reliable information of the HC matrix to the CA matrix and complementing the HC matrix according to the CA matrix simultaneously, the proposed method generates an enhanced CA matrix for better clustering. Technically, the proposed model is formulated as a symmetric constrained convex optimization problem, which is efficiently solved by an alternating iterative algorithm with convergence and global optimum theoretically guaranteed. Extensive experimental comparisons with twelve state-of-the-art methods on eight benchmark datasets substantiate the effectiveness, flexibility and efficiency of the proposed model in ensemble clustering. The codes and datasets can be downloaded at <https://github.com/Siritao/EC-CMS>.

**Index Terms**—Ensemble clustering, Co-association matrix.

## I. INTRODUCTION

**C**LUSTERING is an important unsupervised machine learning task that divides samples into a set of groups to exploit their intrinsic patterns. In the past few years many clustering methods have been proposed, like  $K$ -means [1], [2], mean-shift [3], hierarchical clustering [2], Gaussian mixture models [4], spectral clustering [5], deep embedding clustering [6], and so on. Different clustering methods have their own benefits and drawbacks, and usually consist of several hyper-parameters, which may fit different kinds of problems. However, how to select an appropriate clustering method for a specific problem and how to determine the hyper-parameters of the selected clustering method are still quite challenging. To this end, ensemble clustering (also known as consensus clustering) [7] was proposed to remedy this issue. Specifically, ensemble clustering first generates a set of clustering results by different clustering methods or by a typical clustering method with different hyper-parameters and initializations, and then integrates those base clustering results to generate a consensus one, which is stronger than all the base clusterings.

Y. Jia is with the School of Computer Science and Engineering, Southeast University, Nanjing 210096, China; S. Tao is with the School of Automation, Southeast University, Nanjing 210096, China; R. Wang is with the College of Mathematics and Statistics, Shenzhen University, Shenzhen 518060, China; Y.H. Wang is with the Research Center for Big Data Intelligence, Zhejiang Lab, Hangzhou 311121, China. (e-mail: yhjia@seu.edu.cn, siruitao@seu.edu.cn, wangran@szu.edu.cn, wangyh@zhejianglab.com).

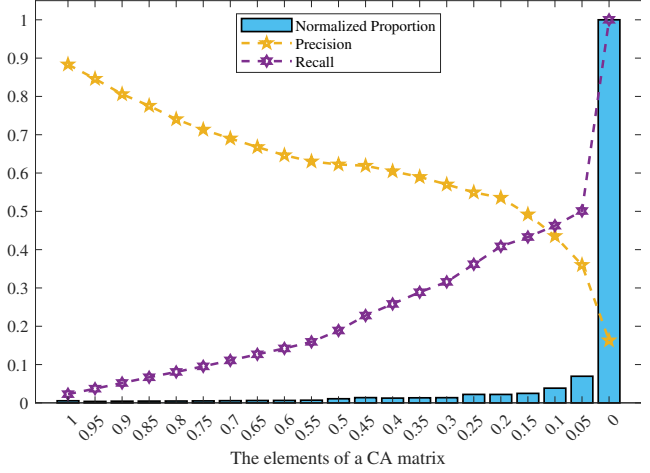


Fig. 1. First,  $K$ -means was used to generate 20 base clusterings on the Caltech20 dataset [8], and then we produced a classic CA matrix by [9] and recorded the frequencies of every two samples that are partitioned into the same cluster (the elements of the CA matrix). We also calculated the precision and recall for different values in the CA matrix. Note that we normalized the proportion of the elements of the CA matrix for better visualization.

To achieve ensemble clustering, existing methods usually first construct a co-association (CA) matrix that records the co-occurrence relationships of samples, i.e., the frequencies of every pair of samples being grouped into the same cluster by the base clusterings [9]. As the CA matrix reflects the pairwise similarity among samples, it can serve as a similarity matrix or adjacency matrix. Then any typical similarity matrix-based clustering methods like spectral clustering or graph partitioning techniques [7], [10], [11] can be applied on the CA matrix to generate the ensemble clustering result. Recently, many efforts have been made to improve the quality of the classic co-occurrence CA matrix based on different priors and assumptions. For example, Li and Ding [12] globally weighted the CA matrix by ranking the quality of each base clustering result. Huang *et al.* [8] proposed the locally weighted CA (LWCA) matrix with an ensemble-driven cluster uncertainty estimation and the local weighting strategy. In PTA [13], the must-link relations among samples rather than all the individual links were focused on so they built a microcluster-based CA (MCA) matrix that is smaller in scale. Some methods assume that the learned CA matrix holds a  $K$ -block-diagonal structure with  $K$  being the number of clusters. For instance, Zhou *et al.* [14] used the Ky Fan's theorem [15] to seek it and designed the CA matrix by self-paced learning, and further extended it to bipartite graph [16]. Zhou *et al.* [17] tried to construct a robust CA matrix by multiple graph

learning. Apart from them, many approaches learned CA matrices with the low-rank assumption. Yi *et al.* [18] viewed reliable relations between samples as observed information and used the matrix completion technique to recover a low-rank CA matrix. Zhou *et al.* [19] proposed to learn a robust and low-rank CA matrix by minimizing the Kullback–Leibler divergence. Tao *et al.* [20] learned a robust CA matrix with low-rank representation to seek the block-diagonal appearance of the CA matrix. Although these methods can improve the clustering performance to some extent, if the used priors are not appropriate for specific tasks, the improvement will be degraded.

To further improve the clustering performance, in this paper we propose a CA matrix self-enhancement method to strengthen the quality of the CA matrix, without any extra information. We found that in a CA matrix, a higher (resp. lower) value provides more (resp. less) reliable description about the pairwise relationship between two samples, while unfortunately, the majority of the elements in a CA matrix have low values. Fig. 1 vividly shows this observation. Motivated by this phenomenon, we first extract the high-confidence information from the base clustering results to constitute a sparse HC matrix, which provides limited but highly-reliable pairwise descriptions of samples. Thereafter, we leverage the HC matrix and the original CA matrix to learn an ideal CA matrix. Specifically, for the HC matrix, we propose to propagate its information to the ideal CA matrix, while for the original CA matrix with many low-reliable but relatively dense connections, we try to denoise it to recover an ideal one. By simultaneously using the information in the HC matrix and the original CA matrix, we are able to learn an enhanced CA matrix with relatively dense connections and more highly-reliable information. The proposed model is finally formulated as a Laplacian-regularized convex optimization problem, and we develop an efficient iterative optimization method to solve it with convergence and global optimum theoretically guaranteed. Extensive experiments on eight benchmark datasets validate its excellent clustering performance when compared with twelve recent ensemble clustering methods. Moreover, the proposed model can adapt to multiple CA matrices and runs faster than most state-of-the-art methods with an iterative optimization process.

The structure of this paper is organized as follows. We first review related works in Section II, thereafter we introduce the proposed model with its numerical solution in Section III. Section IV presents the experimental results and associated analysis, and Section V summarizes this paper.

## II. RELATED WORK

Given  $n$  samples  $\mathcal{X} = \{\mathbf{x}_1, \dots, \mathbf{x}_n\}$  and  $m$  base clustering results  $\boldsymbol{\Pi} = \{\boldsymbol{\pi}_1, \dots, \boldsymbol{\pi}_m\}$ , where  $\mathbf{x}_i$  denotes the  $i$ -th sample and  $\boldsymbol{\pi}_i$  denotes the  $i$ -th base clustering that partitions  $\mathcal{X}$  into several clusters  $\mathcal{C}^i = \{\mathbf{c}_1^i, \dots, \mathbf{c}_{l_i}^i\}$  with  $l_i$  being the number of clusters in  $\mathcal{C}^i$ . According to [9], we can construct a co-occurrence CA matrix  $\tilde{\mathbf{A}} \in \mathbb{R}^{n \times n}$  by

$$\tilde{\mathbf{A}}_{ij} = \frac{1}{m} \sum_{k=1}^m \delta(\mathbf{c}^k(\mathbf{x}_i), \mathbf{c}^k(\mathbf{x}_j)), \quad (1)$$

where  $\mathbf{c}^k(\mathbf{x}_i) \in \mathcal{C}^k$  is the cluster membership of  $\mathbf{x}_i$  in the  $k$ -th base clustering  $\boldsymbol{\pi}_k$ , and  $\delta(\cdot, \cdot)$  is an indicator function:

$$\delta(x, y) = \begin{cases} 1, & x = y \\ 0, & x \neq y \end{cases}$$

As  $\tilde{\mathbf{A}}_{ij}$  measures the frequency that  $\mathbf{x}_i$  and  $\mathbf{x}_j$  occur in the same cluster, it reveals the pairwise similarity between them according to the base clusterings  $\boldsymbol{\Pi}$ . Fred and Jain [9] apply hierarchical agglomerative clustering on the CA matrix to produce a consensus clustering result, which is known as evidence accumulation clustering (EAC). Hereafter, CA-based methods have become the mainstream of ensemble clustering due to their effectiveness and efficiency, and many advanced CA matrix construction methods were proposed [8], [12]–[14], [16]–[20]. In the following, we will introduce two representative ones.

### A. Locally Weighted Co-association

Locally weighted ensemble clustering [8] refines the CA matrix by focusing on local diversity and cluster uncertainty. First, the uncertainty of a given cluster  $\mathbf{c}_s^i$  from  $\boldsymbol{\pi}_i$  is estimated by the entropy, i.e.,

$$U^{\boldsymbol{\Pi}}(\mathbf{c}_s^i) = - \sum_{j=1}^m \sum_{k=1}^{l_j} p(\mathbf{c}_s^i, \mathbf{c}_k^j) \log_2 p(\mathbf{c}_s^i, \mathbf{c}_k^j).$$

Then the ensemble-driven cluster index (ECI) comes up to measure the reliability of a cluster which is negatively correlated with this entropy by a hyper-parameter  $\theta$ :

$$ECI(\mathbf{c}_s^i) = e^{-\frac{U^{\boldsymbol{\Pi}}(\mathbf{c}_s^i)}{\theta \cdot m}}.$$

Finally, the ECIs of all clusters are applied as local weights to compute a locally weighted CA (LWCA) matrix  $\mathbf{A} \in \mathbb{R}^{n \times n}$ :

$$\mathbf{A}_{ij} = \frac{1}{m} \sum_{k=1}^m \delta(\mathbf{c}^k(\mathbf{x}_i), \mathbf{c}^k(\mathbf{x}_j)) \cdot ECI(\mathbf{c}^k(\mathbf{x}_i)).$$

After building the LWCA matrix, hierarchical clustering or Tcut graph partitioning [11] is adopted to generate the final partition.

### B. Microcluster Based Co-association and Probability Trajectory Similarity

Probability trajectory accumulation (PTA) [13] first forms a compact microcluster-based CA (MCA) matrix. Specifically, if all the base clustering assign a group of samples into one cluster, PTA will treat those samples indistinguishably, and aggregate them into a microcluster, which replaces those individual samples in the follow-up steps. PTA creates  $n'$  non-overlapping microclusters  $\mathcal{Y} = \{\mathbf{y}_1, \dots, \mathbf{y}_{n'}\}$ , with each microcluster  $\mathbf{y}_i$  containing  $r_i$  samples. The MCA matrix  $\mathbf{A}' \in \mathbb{R}^{n' \times n'}$  records the frequencies that every two microclusters occur in the same cluster from  $m$  base clustering results  $\boldsymbol{\Pi}$ :

$$\mathbf{A}'_{ij} = \frac{1}{m} \sum_{k=1}^m \delta(\mathbf{c}^k(\mathbf{y}_i), \mathbf{c}^k(\mathbf{y}_j)),$$

where  $\mathbf{c}^k(\mathbf{y}_i) \in \mathcal{C}^k$  is the cluster that  $\pi_k$  assigns microcluster  $\mathbf{y}_i$  to.

Afterwards, PTA proposes an elite neighbor selection strategy to improve the quality of MCA. Specifically, a sparse similarity graph  $\mathbf{W} = \{w_{ij}\} \in \mathbb{R}^{n' \times n'}$  is obtained by reserving the top- $V$  ( $V$  is a hyper-parameter) links of each node and pruning other links, then random walk is conducted on  $\mathbf{W}$  to produce a dense similarity matrix. Considering that the transition probability from a node to another may be proportional to the size of microclusters and the weight of their link, the transition probability matrix  $\mathbf{Q} = \{q_{ij}\} \in \mathbb{R}^{n' \times n'}$  can be calculated by:

$$q_{ij} = \frac{r_j w_{ij}}{\sum_{i \neq k} r_k w_{ik}}.$$

Based on this, the  $T$ -step transition probability from  $\mathbf{y}_i$  to  $\mathbf{y}_j$  is represented by  $[\mathbf{Q}^T]_{ij}$ , and the probability trajectory of a random walker from node  $\mathbf{y}_i$  with step length  $T$  is defined as a  $Tn'$ -tuple  $\mathbf{R}_i = \{\mathbf{Q}_{i,:}^1, \dots, \mathbf{Q}_{i,:}^T\}$ , where  $\mathbf{Q}_{i,:}^T$  denotes the  $i$ -th row in  $\mathbf{Q}^T$ . The final probability trajectory similarity (PTS, also can be regarded as an advanced CA matrix) between two microclusters is the cosine similarity of their probability trajectory, i.e.,

$$\mathbf{A}_{ij} = \frac{\langle \mathbf{R}_i, \mathbf{R}_j \rangle}{\sqrt{\langle \mathbf{R}_i, \mathbf{R}_i \rangle \cdot \langle \mathbf{R}_j, \mathbf{R}_j \rangle}},$$

where  $\langle \cdot, \cdot \rangle$  denotes the inner product operation.

The PTS matrix serves as a similarity measure among microclusters. After applying hierarchical clustering or Tcut on it, the ensemble clustering result can be generated by mapping microclusters back to objects.

As the CA matrix plays a crucial role in ensemble clustering, in this work, we investigate how to improve its quality without additional information.

### III. PROPOSED METHOD

#### A. Formulation

In this section, we will present a novel CA matrix self-enhancement approach to promoting different kinds of CA matrices, and accordingly produce better ensemble clustering performance. From Fig. 1 we can see that in a typical CA matrix, when the majority base clusterings group two samples in the same cluster, those two samples are very likely to belong to the same class (with a high precision), but the total amount of this highly-reliable information is limited (with a low recall). On the contrary, there are a lot of low-value elements (with a high recall) in the CA matrix, which means the base clusterings provide relatively inconsistent description (with a low precision) about two samples. Apparently there exists a complementary relationship between those two kinds of information. As an ideal CA matrix is expected to be filled with dense and highly-reliable elements, we therefore, propose to leverage these two complementary information to enhance a given CA matrix  $\mathbf{A}$ <sup>1</sup>.

<sup>1</sup>Note that here  $\mathbf{A}$  is a general similarity matrix that may have many concrete forms like the classic co-occurrence CA matrix proposed by Fred and Jain [9], or LWCA [8], PTS [13], etc. These similarity matrices can all be enhanced via our model, see related results in Section IV-C.

We first define a high-confidence (HC) matrix  $\mathbf{H} = \{h_{ij}\} \in \mathbb{R}^{n \times n}$  to capture the limited but highly-reliable information from base clusterings  $\Pi$ , i.e.,

$$\mathbf{H} = \Psi_\Omega(\tilde{\mathbf{A}}), \quad (2)$$

where  $\Omega = \{(i, j) \mid \tilde{\mathbf{A}}_{ij} \geq \alpha\}$  records the locations of the highly-reliable elements and  $\Psi_\Omega : \mathbb{R}^{n \times n} \rightarrow \mathbb{R}^{n \times n}$  is a element-wise mapping operator:

$$[\Psi_\Omega(\tilde{\mathbf{A}})]_{ij} = \begin{cases} \tilde{\mathbf{A}}_{ij}, & (i, j) \in \Omega \\ 0, & (i, j) \notin \Omega. \end{cases}$$

Here  $\tilde{\mathbf{A}}$  is the classic CA matrix described in Eq. (1), which directly captures the co-occurrence relationships among samples from base clustering results. If the ratio of the times that two samples  $\mathbf{x}_i$  and  $\mathbf{x}_j$  are grouped into the same class to the total number of base clusterings exceeds a predefined threshold  $\alpha \in [0, 1]$ , the corresponding entry  $\tilde{\mathbf{A}}_{ij}$  is viewed as a piece of highly-reliable information (as well as an element in the HC matrix).

Second, we would directly use the given input CA matrix  $\mathbf{A}$  to depict the relatively low-reliable information. Accordingly, *CA matrix self-enhancement becomes using  $\mathbf{H}$  and  $\mathbf{A}$  to recover an ideal CA matrix  $\mathbf{C} \in \mathbb{R}^{n \times n}$ .*

As  $\mathbf{A}$  may contain many inaccurate information, which can be regarded as the combination of the ideal CA matrix with noise. We therefore, try to remove the noise from  $\mathbf{A}$  to construct  $\mathbf{C}$ , i.e.,

$$\begin{aligned} \min_{\mathbf{C}, \mathbf{E}} \quad & \|\mathbf{E}\|_F^2 \\ \text{s.t.} \quad & \mathbf{A} = \mathbf{C} + \mathbf{E}, \quad \mathbf{C} = \mathbf{C}^\top, \quad \mathbf{0} \leq \mathbf{C} \leq \mathbf{1}, \end{aligned} \quad (3)$$

where  $\mathbf{E} \in \mathbb{R}^{n \times n}$  denotes the error term and  $\|\cdot\|_F$  denotes the Frobenius norm of a matrix. Ideally,  $\mathbf{C}$  should be symmetric because if  $\mathbf{x}_i$  is similar to  $\mathbf{x}_j$ ,  $\mathbf{x}_j$  should also be similar to  $\mathbf{x}_i$ . Besides, with  $\mathbf{C}_{i,j}$  being the similarity measure, its value should lies in  $[0, 1]$ .

However, solving Eq. (3) will lead to a trivial solution, i.e.,  $\mathbf{C} = \mathbf{A}$  and  $\mathbf{E} = \mathbf{0}$ . To avoid this, it is significant to further propagate the limited but highly valuable information from  $\mathbf{H}$  to help build a reasonable  $\mathbf{C}$ . Let  $\mathbf{C}_{i,:}$  denotes the  $i$ -th row of matrix  $\mathbf{C}$ , which can reflect the pairwise similarity relationships of  $\mathbf{x}_i$  with the other samples. If  $h_{ij} > 0$ ,  $\mathbf{x}_i$  and  $\mathbf{x}_j$  are very likely to belong to the same cluster. Accordingly, the pairwise relationships of  $\mathbf{x}_i$  with the other samples should also be close to that of  $\mathbf{x}_j$ , i.e., when  $h_{i,j} > 0$ , we can infer that  $\mathbf{C}_{i,:}$  should be close to  $\mathbf{C}_{j,:}$ . The intuition to minimize row-wise discrepancies w.r.t. every pair of samples that potentially belong to the same cluster can be mathematically expressed as:

$$\min_{\mathbf{C}} \quad \sum_{i,j=1}^n h_{ij} \|\mathbf{C}_{i,:} - \mathbf{C}_{j,:}\|_2^2.$$

In addition, if  $h_{ij} > 0$ , we can expect that  $\mathbf{A}_{ij}$  is accurate enough to represent the pairwise similarity between  $\mathbf{x}_i$  and  $\mathbf{x}_j$ . We thus copy those crucial entries of  $\mathbf{A}$  to  $\mathbf{C}$  directly, which would serve as the supporter of the co-association structure. Taking all the above analyses into consideration, the proposed model is further formulated as:

**Algorithm 1** Ensemble Clustering via Co-association Matrix Self-enhancement

**Input:** CA matrix  $\mathbf{A}$ , base clusterings  $\Pi$ , threshold  $\alpha$ , trade-off parameter  $\lambda$ .

**Initialization:** Penalty parameter  $\gamma_1 = \gamma_2 = 1$ , tolerance  $\epsilon = 1e - 2$ ,  $k = 0$ ,  $\mathbf{E}_k = \mathbf{C}_k = \mathbf{F}_k = \mathbf{0} \in \mathbb{R}^{n \times n}$ ,  $\mathbf{Y}_{1k} = \mathbf{A} - \mathbf{C}_k - \mathbf{E}_k$ ,  $\mathbf{Y}_{2k} = \mathbf{C}_k - \mathbf{F}_k$ .

- 1: Construct the co-occurrence CA matrix  $\tilde{\mathbf{A}}$  by Eq. (1) from  $\Pi$ , then generate the HC indices set  $\Omega$  and derive the HC matrix  $\mathbf{H}$  via Eq. (2).
- 2: Compute  $\Phi = \text{diag}[\mathbf{H} \cdot (\mathbf{1} \in \mathbb{R}^n)] - \mathbf{H}$ .
- 3: **while** not converged **do**
- 4:   Update  $\mathbf{C}_{k+1}$  via Eq. (9).
- 5:   Update  $\mathbf{E}_{k+1}$  via Eq. (11).
- 6:   Update  $\mathbf{F}_{k+1}$  via Eq. (13).
- 7:   Update  $\mathbf{Y}_{1(k+1)}$ ,  $\mathbf{Y}_{2(k+1)}$  via Eq. (14).
- 8:   Check stopping criteria:  

$$\max(\sigma_k(\mathbf{C}), \sigma_k(\mathbf{E}), \sigma_k(\mathbf{F}), \sigma_k(\mathbf{Y}_1), \sigma_k(\mathbf{Y}_2)) \leq \epsilon$$
with  $\sigma_k(\mathbf{C}) = (\|\mathbf{C}_{k+1} - \mathbf{C}_k\|_F^2)/\|\mathbf{C}_k\|_F^2$ .
- 9:    $k \leftarrow k + 1$ .
- 10: **end while**
- 11: **return** the enhanced CA matrix  $\mathbf{C}$ .

$$\begin{aligned} \min_{\mathbf{C}, \mathbf{E}} \quad & \frac{1}{2} \sum_{i,j=1}^n h_{ij} \|\mathbf{C}_{i,:} - \mathbf{C}_{j,:}\|_2^2 + \frac{\lambda}{2} \|\mathbf{E}\|_F^2 \\ \text{s.t.} \quad & \mathbf{A} = \mathbf{C} + \mathbf{E}, \mathbf{C}_{ij} = \mathbf{A}_{ij}, \forall (i, j) \in \Omega, \\ & \mathbf{C} = \mathbf{C}^\top, \mathbf{0} \leq \mathbf{C} \leq \mathbf{1}, \end{aligned} \quad (4)$$

where  $\lambda > 0$  balances the two loss terms. The first term can be written in a quadratic form  $\text{tr}(\mathbf{C}^\top \Phi \mathbf{C})$  [21], where  $\Phi = \mathbf{D} - \mathbf{H}$  is the graph Laplacian matrix, and  $\mathbf{D}$  is the diagonal degree matrix with its diagonal element  $\mathbf{D}_{ii} = \sum_j \mathbf{H}_{ij}$ . Also, operator  $\Psi_\Omega$  can be assigned to matrix  $\mathbf{E}$  to compensate for unknown entries of  $\mathbf{A}$  but locks  $\mathbf{C}_{ij} = \mathbf{A}_{ij}$  for  $(i, j) \in \Omega$ . Finally, the proposed model is re-written as:

$$\begin{aligned} \min_{\mathbf{C}, \mathbf{E}} \quad & \text{tr}(\mathbf{C}^\top \Phi \mathbf{C}) + \frac{\lambda}{2} \|\mathbf{E}\|_F^2 \\ \text{s.t.} \quad & \mathbf{A} = \mathbf{C} + \mathbf{E}, \Psi_\Omega(\mathbf{E}) = \mathbf{0}, \mathbf{C} = \mathbf{C}^\top, \mathbf{0} \leq \mathbf{C} \leq \mathbf{1}. \end{aligned} \quad (5)$$

As a summary, Eq. (5) propagates the highly-reliable information in  $\mathbf{H}$  and removes the noise in  $\mathbf{A}$  simultaneously to learn an enhanced CA matrix  $\mathbf{C}$  without any extra information. It can be applied to enhance different kinds of CA matrices (or similarity matrices) like  $\tilde{\mathbf{A}}$ , LWCA, PTS, etc. After solving Eq. (5), average-link hierarchical agglomerative clustering is applied on  $\mathbf{C}$  to obtain the final clustering result. Other clustering approaches like spectral clustering are also applicable here.

## B. Optimization

We adopt the Alternating Direction Method of Multipliers (ADMM) method [22] to solve Eq. (5), which can handle the equality constraint and the multiple variables effectively. In order to alleviate the value range constraint and the symmetric

constraint of  $\mathbf{C}$ , we introduce an intermediate matrix  $\mathbf{F}$  to shoulder them, and equivalently re-write Eq. (5) as

$$\begin{aligned} \min_{\mathbf{C}, \mathbf{E}, \mathbf{F}} \quad & \text{tr}(\mathbf{C}^\top \Phi \mathbf{C}) + \frac{\lambda}{2} \|\mathbf{E}\|_F^2 \\ \text{s.t.} \quad & \mathbf{A} = \mathbf{C} + \mathbf{E}, \Psi_\Omega(\mathbf{E}) = \mathbf{0}, \mathbf{C} = \mathbf{F}, \\ & \mathbf{F} = \mathbf{F}^\top, \mathbf{0} \leq \mathbf{F} \leq \mathbf{1}. \end{aligned} \quad (6)$$

Let  $\mathbf{Y}_1$  and  $\mathbf{Y}_2$  denote the Lagrangian multipliers, the augmented Lagrangian function of Eq. (6) can be written as:

$$\begin{aligned} \mathcal{L}(\mathbf{C}, \mathbf{E}, \mathbf{F}, \mathbf{Y}_1, \mathbf{Y}_2) = & \text{tr}(\mathbf{C}^\top \Phi \mathbf{C}) + \frac{\lambda}{2} \|\mathbf{E}\|_F^2 \\ & + \langle \mathbf{Y}_1, \mathbf{A} - \mathbf{C} - \mathbf{E} \rangle + \frac{\gamma_1}{2} \|\mathbf{A} - \mathbf{C} - \mathbf{E}\|_F^2 \\ & + \langle \mathbf{Y}_2, \mathbf{C} - \mathbf{F} \rangle + \frac{\gamma_2}{2} \|\mathbf{C} - \mathbf{F}\|_F^2 \\ \text{s.t.} \quad & \Psi_\Omega(\mathbf{E}) = \mathbf{0}, \mathbf{F} = \mathbf{F}^\top, \mathbf{0} \leq \mathbf{F} \leq \mathbf{1}, \end{aligned} \quad (7)$$

where  $\gamma_1, \gamma_2 > 0$  introduce the augmented Lagrangian term. The solution to Eq. (5) can be obtained when Eq. (7) reaches its minimum. Specifically, Eq. (7) can be solved by the following iterative alternating procedures.

1) *Updating  $\mathbf{C}$ :* With other variables fixed, the  $\mathbf{C}$  sub-problem is formulated as:

$$\begin{aligned} \mathbf{C}_{k+1} = & \arg \min_{\mathbf{C}} \text{tr}(\mathbf{C}^\top \Phi \mathbf{C}) + \frac{\gamma_1}{2} \|\mathbf{C} - \mathbf{P}_{1k}\|_F^2 \\ & + \frac{\gamma_2}{2} \|\mathbf{C} - \mathbf{P}_{2k}\|_F^2, \end{aligned} \quad (8)$$

where  $\mathbf{P}_{1k} = \mathbf{A} - \mathbf{E}_k + \mathbf{Y}_{1k}/\gamma_1$  and  $\mathbf{P}_{2k} = \mathbf{F}_k - \mathbf{Y}_{2k}/\gamma_2$ . By setting the derivative of Eq. (8) to 0, we have the following analytical solution of the  $\mathbf{C}$  sub-problem:

$$\mathbf{C}_{k+1} = (2\Phi + (\gamma_1 + \gamma_2)\mathbf{I})^{-1} (\gamma_1 \mathbf{P}_{1k} + \gamma_2 \mathbf{P}_{2k}). \quad (9)$$

2) *Updating  $\mathbf{E}$ :* With other variables fixed, the formulation of the  $\mathbf{E}$  sub-problem is:

$$\begin{aligned} \mathbf{E}_{k+1} = & \arg \min_{\mathbf{E}} \frac{\gamma_1}{2} \|\mathbf{E} - (\mathbf{A} - \mathbf{C}_{k+1})\|_F^2 + \frac{\lambda}{2} \|\mathbf{E}\|_F^2 \\ & + \langle \mathbf{Y}_{1k}, \mathbf{A} - \mathbf{C}_{k+1} - \mathbf{E} \rangle \\ \text{s.t.} \quad & \Psi_\Omega(\mathbf{E}) = \mathbf{0}. \end{aligned} \quad (10)$$

As the Frobenius norm, the inner product and the equality constraint are all computed element-wisely, we can get the global solution of Eq. (10) through:

$$\mathbf{E}^* = \frac{\gamma_1(\mathbf{A} - \mathbf{C}_{k+1}) + \mathbf{Y}_{1k}}{\lambda + \gamma_1}, \quad \mathbf{E}_{k+1} = \Psi_{\bar{\Omega}}(\mathbf{E}^*), \quad (11)$$

where  $\bar{\Omega}$  is the complementary set of  $\Omega$ .

3) *Updating  $\mathbf{F}$ :* With other variables fixed, the  $\mathbf{F}$  sub-problem can be expressed as:

$$\begin{aligned} \mathbf{F}_{k+1} = & \arg \min_{\mathbf{F}} \frac{1}{2} \|\mathbf{F} - \mathbf{P}_{3k}\|_F^2 \\ \text{s.t.} \quad & \mathbf{F} = \mathbf{F}^\top, \mathbf{0} \leq \mathbf{F} \leq \mathbf{1}, \end{aligned} \quad (12)$$

where  $\mathbf{P}_{3k} = \mathbf{C}_{k+1} + \mathbf{Y}_{2k}/\gamma_2$ . Since  $\mathbf{F} = \mathbf{F}^\top$  suggests that  $\|\mathbf{F} - \mathbf{P}_{3k}\|_F^2 = \|\mathbf{F} - \mathbf{P}_{3k}^\top\|_F^2$ , Eq. (12) is equivalent to:

$$\begin{aligned} \mathbf{F}_{k+1} = & \arg \min_{\mathbf{F}} \frac{1}{4} (\|\mathbf{F} - \mathbf{P}_{3k}\|_F^2 + \|\mathbf{F} - \mathbf{P}_{3k}^\top\|_F^2) \\ = & \arg \min_{\mathbf{F}} \frac{1}{2} \left\| \mathbf{F} - \frac{\mathbf{P}_{3k} + \mathbf{P}_{3k}^\top}{2} \right\|_F^2 + c(\mathbf{P}) \\ \text{s.t.} \quad & \mathbf{F} = \mathbf{F}^\top, \mathbf{0} \leq \mathbf{F} \leq \mathbf{1}. \end{aligned}$$

TABLE I  
DESCRIPTION OF THE DATASETS.

Dataset	#Instance	#Feature	#Class	Source
Caltech20	2,386	30,000	20	IMAGE, [8], [23]
Ecoli	336	8	8	UCI
LS	6,435	36	6	UCI
FCT	3,780	54	7	UCI
Aggregation	788	2	7	UCI
Texture	5,500	40	11	UCI
UMIST	575	644	20	FACE, [24]
SPF	1,941	27	7	UCI

with  $c(\mathbf{P})$  irrelevant to  $\mathbf{F}$ . Thereafter, the optimum of Eq. (12) is achieved through an element-wisely truncation:

$$\mathbf{F}_{k+1} = \min \left( \max \left( \frac{\mathbf{P}_{3k} + \mathbf{P}_{3k}^\top}{2}, 0 \right), 1 \right). \quad (13)$$

4) *Updating  $\mathbf{Y}$ :* The ADMM algorithm updates the multiplier matrices  $\mathbf{Y}_1$ ,  $\mathbf{Y}_2$  by:

$$\begin{aligned} \mathbf{Y}_{1(k+1)} &= \mathbf{Y}_{1k} + \gamma_1 (\mathbf{A} - \mathbf{C}_{k+1} - \mathbf{E}_{k+1}), \\ \mathbf{Y}_{2(k+1)} &= \mathbf{Y}_{2k} + \gamma_2 (\mathbf{C}_{k+1} - \mathbf{F}_{k+1}). \end{aligned} \quad (14)$$

The whole procedure is summarized in Algorithm 1. As Eq. (5) is a convex problem with two blocks of variables (i.e.,  $\{\mathbf{C}\}$  and  $\{\mathbf{E}, \mathbf{F}\}$ ), since updating variables  $\mathbf{E}$  and  $\mathbf{F}$  are independent of each other), Algorithm 1 is theoretically guaranteed to converge to a global solution by ADMM [22].

### C. Computational Complexity Analysis

Updating  $\mathbf{C}$  involves a matrix inverse operation and a matrix multiplication operation. As in each iteration, the to-be-inversed matrix  $2\Phi + (\gamma_1 + \gamma_2)\mathbf{I}$  is fixed so that can be calculated in advance, which means the computational complexity of solving the  $\mathbf{C}$  sub-problem is  $\mathcal{O}(n^{2.37})$  [25]. Solving sub-problems of  $\mathbf{E}$ ,  $\mathbf{F}$  and updating multiplier matrices  $\mathbf{Y}_1$ ,  $\mathbf{Y}_2$  only include element-wise calculations, leading to a computational complexity of  $\mathcal{O}(n^2)$ . Therefore, the overall computational complexity of Algorithm 1 is  $\mathcal{O}(n^{2.37})$  in one iteration.

## IV. EXPERIMENT

We conducted a series of experiments on eight real-world benchmark datasets to verify the effectiveness of the proposed algorithm, whose detailed information is summarized in Table I. Following Huang *et al.* [8], for all the datasets, 100 candidate base clusterings were generated by  $K$ -means with  $K$  randomly selecting in  $[2, \sqrt{n}]$  and  $n$  being the number of samples.

We compared the proposed method with twelve representative state-of-the-art ensemble clustering algorithms, which are listed as follows.

- 1) PTA-AL, PTA-CL, PTGP [13]: three microcluster representation-based ensemble clustering methods using similarity matrix derived from probability trajectories of random walkers. They adopt average-link (AL) hierarchical agglomerative clustering, complete-link (CL) hierarchical agglomerative clustering and Tcut graph

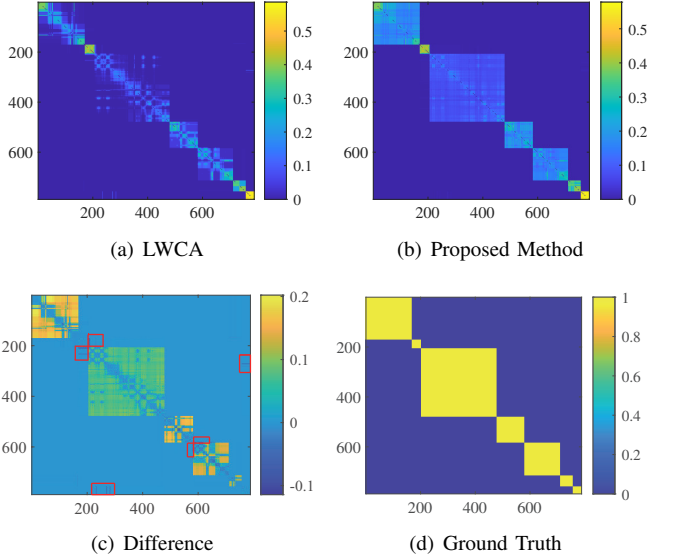


Fig. 2. Comparison of the LWCA, the proposed CA matrix, their difference and the ideal one produced by ground truth labels.

partitioning (GP) [11] respectively to generate clustering results.

- 2) LWEA, LWGP [8]: Two locally-weighted ensemble clustering methods with average-link hierarchical agglomerative clustering and Tcut, corresponding to LWEA (evidence accumulation) and LWGP (graph partitioning). The local weights are obtained via an ensemble-driven cluster uncertainty estimation.
- 3) RSEC-H, RSEC-Z [20]: robust spectral ensemble clustering methods via rank minimization. The algorithm simultaneously learns a consensus partition  $\mathbf{H}$  and a low-rank representation  $\mathbf{Z}$ , and respectively adopts  $K$ -means or spectral clustering on them to get final results.
- 4) DREC [26]: a dense representation-based ensemble clustering algorithm. It also uses the idea of forming microclusters but with the consideration of outliers.
- 5) SPCE [14]: ensemble clustering with a self-paced manner. It learns a CA matrix from easy-to-learn samples to difficult-to-learn ones.
- 6) ECPCS-MC, ECPCS-HC [27]: two ensemble clustering methods that improve the CA matrix by propagating cluster-wise similarities. Here, MC refers to cluster-level meta-clustering and HC refers to average-link hierarchical agglomerative clustering.
- 7) TRCE [17]: a multiple graph learning-based ensemble clustering method combining three levels of robustness, i.e., base clustering level, graph level and instance level.

For a fair comparison, we carefully tuned the hyper-parameters of those compared methods according to their original papers and reported the best performances. As for the proposed method, the LWCA matrix [8] was employed as the input CA matrix. For all the methods, we randomly selected 20 base clusterings from the candidate base clustering pool and recorded the average clustering performance with the standard deviation over 20 repetitions. All experiments were conducted

TABLE II

CLUSTERING PERFORMANCES OF DIFFERENT ALGORITHMS MEASURED BY ARI, WHERE THE BEST PERFORMANCE AND THE SECOND BEST ONE ARE HIGHLIGHTED BY BOLD AND UNDERLINE.

Method	Caltech20	Ecoli	LS	FCT	Aggregation	Texture	UMIST	SPF
Base clusterings (average)	0.209±0.061	0.396±0.120	0.235±0.100	0.075±0.017	0.463±0.171	0.373±0.088	0.273±0.092	0.044±0.013
Base clusterings (best)	0.345	0.695	0.479	0.120	0.822	0.530	0.389	0.073
PTA-AL [TKDE, 2016]	0.356±0.034	0.340±0.043	0.593±0.079	0.136±0.017	0.600±0.128	0.658±0.046	0.323±0.027	0.081±0.015
PTA-CL [TKDE, 2016]	0.334±0.026	0.342±0.045	0.452±0.068	0.124±0.015	0.529±0.181	0.604±0.027	0.323±0.029	0.075±0.018
PTGP [TKDE, 2016]	0.335±0.042	0.351±0.038	0.513±0.040	0.127±0.011	0.633±0.094	0.632±0.044	0.317±0.030	0.079±0.017
LWGP [TCYB, 2018]	0.226±0.019	0.417±0.046	0.590±0.019	0.121±0.011	0.971±0.010	0.658±0.048	0.345±0.020	0.084±0.015
RSEC-H [TKDD, 2019]	0.180±0.027	0.477±0.110	0.475±0.082	0.094±0.030	0.973±0.048	0.445±0.057	0.360±0.046	0.060±0.025
RSEC-Z [TKDD, 2019]	0.201±0.032	0.397±0.149	0.483±0.076	0.100±0.025	0.892±0.080	0.485±0.041	0.325±0.050	0.053±0.023
DREC [Neurocomputing, 2019]	0.257±0.026	0.679±0.079	0.544±0.008	0.126±0.014	0.897±0.076	0.703±0.042	0.367±0.038	0.093±0.014
SPCE [TNNLS, 2021]	0.317±0.106	0.737±0.057	0.475±0.127	0.113±0.037	0.965±0.054	0.578±0.074	0.369±0.039	0.088±0.021
ECPCS-MC [TSMC-S, 2021]	0.271±0.019	0.520±0.039	0.546±0.036	0.113±0.011	0.928±0.068	0.611±0.035	0.328±0.035	0.067±0.005
ECPCS-HC [TSMC-S, 2021]	0.379±0.025	0.731±0.020	0.583±0.076	0.139±0.017	0.981±0.033	0.633±0.052	0.317±0.039	0.067±0.015
TRCE [AAAI, 2021]	0.237±0.028	0.643±0.128	0.588±0.038	0.095±0.022	0.946±0.085	0.621±0.048	0.321±0.043	0.059±0.017
LWEA [TCYB, 2018]	0.367±0.033	0.430±0.030	0.558±0.060	0.130±0.016	0.928±0.096	0.705±0.045	0.348±0.038	0.084±0.018
Proposed	<b>0.525±0.075</b>	<b>0.754±0.018</b>	<b>0.657±0.024</b>	<b>0.179±0.017</b>	<b>0.989±0.004</b>	<b>0.723±0.052</b>	<b>0.371±0.056</b>	<b>0.105±0.022</b>

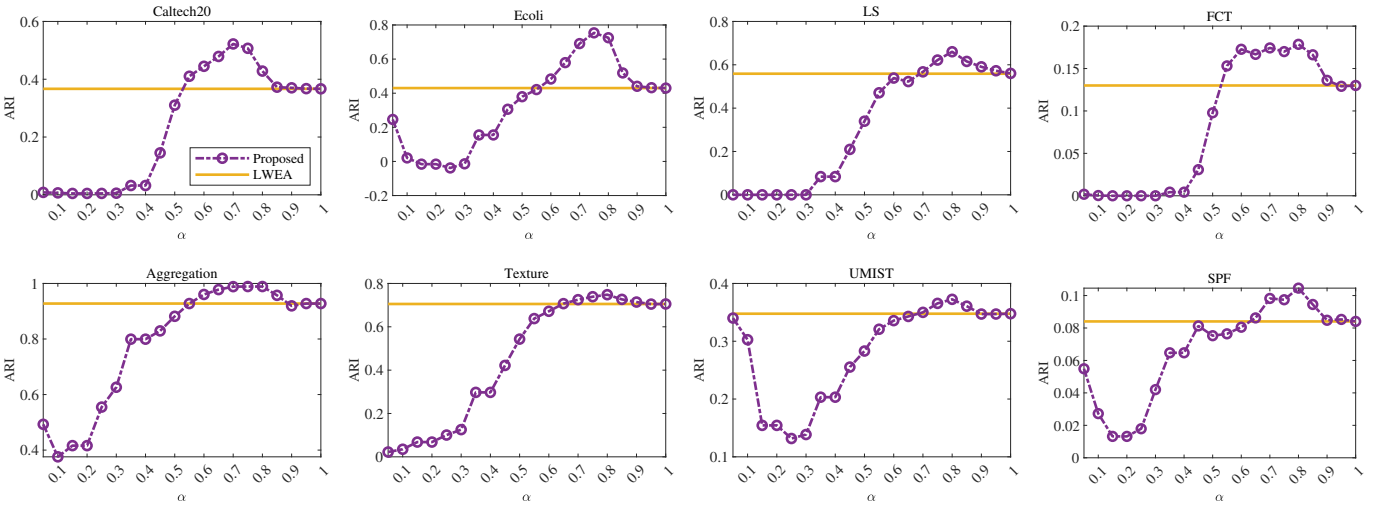


Fig. 3. Clustering performances w.r.t. ARI with varying  $\alpha$ . Both LWEA and the proposed method adopt average-link hierarchical agglomerative clustering on the CA matrix to produce the clustering result. All the sub-figures share the same legend.

by MATLAB R2020a on a PC with 2.3GHz CPU and 16GB memory.

We adopted three widely-used metrics, i.e., adjusted rand index (ARI) [28], normalized mutual information (NMI) [7], F-score (the harmonic mean of precision and recall) to evaluate the clustering performance of different methods. All of them lie in the range of  $[0, 1]$ , and larger values reflect better clustering performance.

#### A. Parameter Sensitivity

There are two hyper-parameters  $\alpha$  and  $\lambda$  in our model, where  $\alpha$  decides to what extent we can accept an entry in the CA matrix  $\mathbf{A}$  as a high-confidence element, and  $\lambda$  balances the importance of the error term. We investigated their influence on the proposed model in Figs. 3 and 4.

- First, it can be seen from Fig. 3 that the optimal performance is achieved when  $\alpha$  is 0.7 on Caltech20, 0.75 on Ecoli and 0.8 on all other datasets. Moreover, an apparent

improvement of our method over the baseline LWEA usually occurs when  $\alpha \in \{0.7, 0.75, 0.8\}$  since a bigger  $\alpha$  will largely reduce the amount of the highly-reliable information, while a smaller  $\alpha$  will degrade the quality of HC matrix.

- Second, from Fig. 4, we can observe that when  $\lambda$  is too large (e.g.,  $\lambda \geq 100$ ), the performance of the proposed model will be close to that of LWEA, as with a large  $\lambda$ , the self-enhanced CA matrix will be close to the original one.  $\lambda$  should also not be too small, as with a small  $\lambda$ , the majority elements of the original CA matrix will be regarded as noise and be removed. Moreover, our model significantly surpasses the baseline on a wide range of  $\lambda$ , i.e.,  $\lambda \in [0.01, 1]$  on most of the datasets, proving its robustness.

As a summary, we suggest setting  $\alpha = 0.8$  and  $\lambda = 0.4$  for our model.

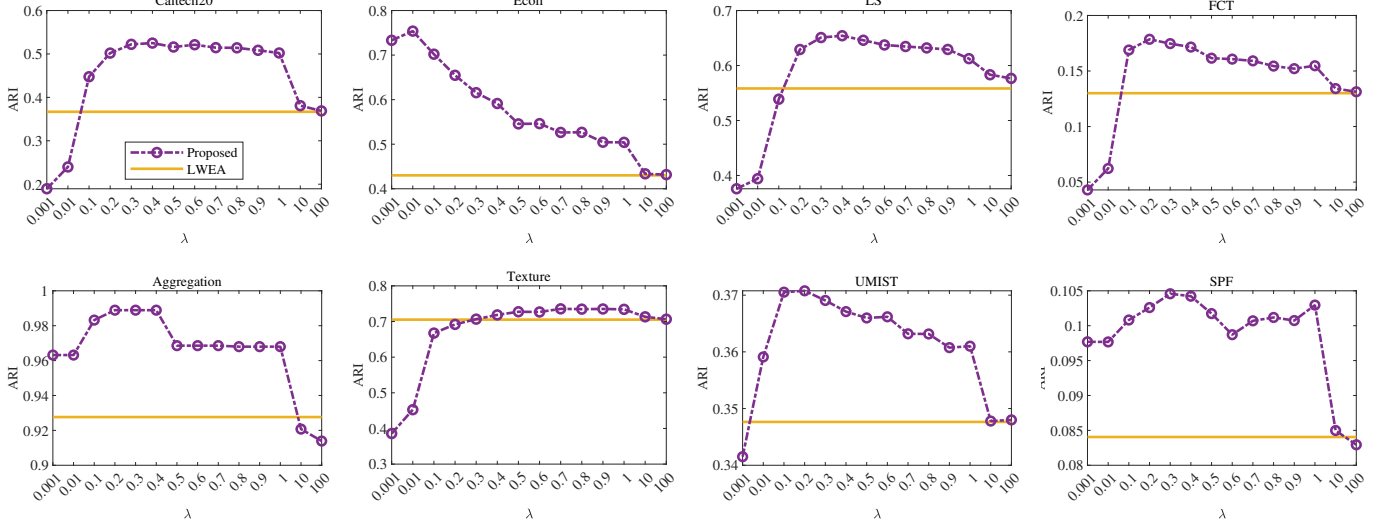


Fig. 4. Clustering performances w.r.t. ARI with varying  $\lambda$ . Both LWEA and the proposed method adopt average-link hierarchical agglomerative clustering on the CA matrix to produce the clustering result. All the sub-figures share the same legend.

TABLE III  
CLUSTERING PERFORMANCES OF DIFFERENT ALGORITHMS MEASURED BY NMI.

Method	Caltech20	Ecoli	LS	FCT	Aggregation	Texture	UMIST	SPF
Base clusterings (average)	0.424 $\pm$ 0.061	0.579 $\pm$ 0.041	0.507 $\pm$ 0.050	0.255 $\pm$ 0.033	0.743 $\pm$ 0.073	0.655 $\pm$ 0.064	0.574 $\pm$ 0.133	0.157 $\pm$ 0.029
Base clusterings (best)	0.478	0.669	0.611	0.290	0.878	0.698	0.705	0.180
PTA-AL [TKDE, 2016]	0.440 $\pm$ 0.006	0.561 $\pm$ 0.023	0.635 $\pm$ 0.033	0.242 $\pm$ 0.018	0.786 $\pm$ 0.066	0.772 $\pm$ 0.025	0.633 $\pm$ 0.026	0.152 $\pm$ 0.019
PTA-CL [TKDE, 2016]	0.436 $\pm$ 0.010	0.560 $\pm$ 0.023	0.568 $\pm$ 0.046	0.234 $\pm$ 0.021	0.745 $\pm$ 0.108	0.730 $\pm$ 0.018	0.633 $\pm$ 0.026	0.136 $\pm$ 0.025
PTGP [TKDE, 2016]	0.431 $\pm$ 0.010	0.566 $\pm$ 0.021	0.614 $\pm$ 0.024	0.237 $\pm$ 0.017	0.800 $\pm$ 0.053	0.747 $\pm$ 0.028	0.629 $\pm$ 0.024	0.151 $\pm$ 0.017
LWGP [TCYB, 2018]	0.453 $\pm$ 0.011	0.613 $\pm$ 0.024	0.659 $\pm$ 0.017	0.227 $\pm$ 0.011	0.968 $\pm$ 0.009	0.774 $\pm$ 0.024	0.659 $\pm$ 0.016	0.152 $\pm$ 0.013
RSEC-H [TKDD, 2019]	0.445 $\pm$ 0.015	0.607 $\pm$ 0.048	0.596 $\pm$ 0.042	0.194 $\pm$ 0.038	0.976 $\pm$ 0.029	0.697 $\pm$ 0.026	0.684 $\pm$ 0.037	0.109 $\pm$ 0.041
RSEC-Z [TKDD, 2019]	0.436 $\pm$ 0.013	0.556 $\pm$ 0.073	0.596 $\pm$ 0.044	0.197 $\pm$ 0.030	0.929 $\pm$ 0.040	0.702 $\pm$ 0.017	0.651 $\pm$ 0.042	0.099 $\pm$ 0.034
DREC [Neurocomputing, 2019]	0.457 $\pm$ 0.009	0.658 $\pm$ 0.053	0.634 $\pm$ 0.004	0.238 $\pm$ 0.018	0.932 $\pm$ 0.040	0.796 $\pm$ 0.022	0.683 $\pm$ 0.027	0.159 $\pm$ 0.010
SPCE [TNNLS, 2021]	0.460 $\pm$ 0.051	0.710 $\pm$ 0.024	0.566 $\pm$ 0.071	0.272 $\pm$ 0.026	0.970 $\pm$ 0.031	0.785 $\pm$ 0.025	<b>0.715<math>\pm</math>0.041</b>	<b>0.212<math>\pm</math>0.015</b>
ECPCS-MC [TSMC-S, 2021]	0.469 $\pm$ 0.007	0.656 $\pm$ 0.017	0.635 $\pm$ 0.016	0.206 $\pm$ 0.012	0.946 $\pm$ 0.033	0.744 $\pm$ 0.019	0.645 $\pm$ 0.040	0.143 $\pm$ 0.011
ECPCS-HC [TSMC-S, 2021]	0.471 $\pm$ 0.019	0.701 $\pm$ 0.018	0.643 $\pm$ 0.043	0.229 $\pm$ 0.017	0.980 $\pm$ 0.017	0.756 $\pm$ 0.029	0.643 $\pm$ 0.037	0.143 $\pm$ 0.018
TRCE [AAAI, 2021]	0.459 $\pm$ 0.010	0.669 $\pm$ 0.048	0.662 $\pm$ 0.012	0.198 $\pm$ 0.014	0.964 $\pm$ 0.040	0.761 $\pm$ 0.028	0.695 $\pm$ 0.021	0.133 $\pm$ 0.021
LWEA [TCYB, 2018]	<b>0.480<math>\pm</math>0.007</b>	0.615 $\pm$ 0.015	0.630 $\pm$ 0.026	0.236 $\pm$ 0.021	0.958 $\pm$ 0.041	0.794 $\pm$ 0.024	0.664 $\pm$ 0.036	0.156 $\pm$ 0.022
Proposed	<b>0.497<math>\pm</math>0.020</b>	<b>0.716<math>\pm</math>0.017</b>	<b>0.685<math>\pm</math>0.015</b>	<b>0.276<math>\pm</math>0.015</b>	<b>0.984<math>\pm</math>0.004</b>	<b>0.811<math>\pm</math>0.022</b>	0.692 $\pm$ 0.068	<b>0.204<math>\pm</math>0.025</b>

### B. Clustering Performance Comparison

Tables II, III, IV show the average ARI, NMI, F-score as well as the standard deviation of the compared and proposed algorithms on all the benchmark datasets. Additionally, the best and average performance of the base clusterings from the candidate base clustering pool are also included. From those tables, we have the following observations.

- First, nearly all the ensemble clustering methods perform better than the average performance of the base clusterings w.r.t. different metrics, which indicates that leveraging multiple base clusterings is useful. But many compared methods cannot exceed the best base clustering on most datasets, e.g., PTA-CL and RSEC-Z, suggesting their limitations. Differently, the proposed method can significantly outperform both the average performance of the base clusterings and the best base clustering in the candidate base clustering pool on most datasets, which proves that the proposed method can really exploit the

useful information from the base clusterings and improve the clustering performance.

- Second, the proposed method takes the CA matrix of LWEA as input, and it can largely improve the clustering performance of LWEA on all the datasets, e.g., on Ecoli, our method improves the ARI from 0.430 to 0.754, NMI from 0.615 to 0.716 and F-score from 0.544 to 0.823. This is a straightforward proof that our method can improve the quality of the input CA matrix.
- Third, the proposed method outperforms all the compared methods on all the datasets w.r.t. ARI and F-score. For example, on Caltech20, the proposed method improves ARI about 40% compared with the best comparison. In terms of NMI, our method achieves the best performance on 6 out of 8 cases, and slightly inferior to SPCE on UMIST and SPF. Taking all the metrics into consideration, we can conclude that the proposed model ranks first in general.

TABLE IV  
CLUSTERING PERFORMANCES OF DIFFERENT ALGORITHMS MEASURED BY F-SCORE.

Method	Caltech20	Ecoli	LS	FCT	Aggregation	Texture	UMIST	SPF
Base clusterings (average)	0.283 $\pm$ 0.082	0.504 $\pm$ 0.127	0.291 $\pm$ 0.121	0.140 $\pm$ 0.057	0.528 $\pm$ 0.174	0.410 $\pm$ 0.086	0.320 $\pm$ 0.076	0.146 $\pm$ 0.064
Base clusterings (best)	0.440	0.780	0.555	0.299	0.865	0.563	0.420	0.348
PTA-AL [TKDE, 2016]	0.436 $\pm$ 0.033	0.460 $\pm$ 0.035	0.673 $\pm$ 0.064	0.271 $\pm$ 0.015	0.681 $\pm$ 0.098	0.691 $\pm$ 0.041	0.361 $\pm$ 0.023	0.261 $\pm$ 0.015
PTA-CL [TKDE, 2016]	0.412 $\pm$ 0.024	0.463 $\pm$ 0.036	0.555 $\pm$ 0.055	0.256 $\pm$ 0.013	0.632 $\pm$ 0.129	0.641 $\pm$ 0.024	0.361 $\pm$ 0.025	0.248 $\pm$ 0.012
PTGP [TKDE, 2016]	0.410 $\pm$ 0.040	0.468 $\pm$ 0.031	0.604 $\pm$ 0.032	0.255 $\pm$ 0.011	0.705 $\pm$ 0.073	0.667 $\pm$ 0.040	0.356 $\pm$ 0.027	0.248 $\pm$ 0.015
LWGP [TCYB, 2018]	0.298 $\pm$ 0.019	0.527 $\pm$ 0.042	0.670 $\pm$ 0.019	0.256 $\pm$ 0.010	0.977 $\pm$ 0.008	0.690 $\pm$ 0.043	0.381 $\pm$ 0.019	0.262 $\pm$ 0.014
RSEC-H [TKDD, 2019]	0.276 $\pm$ 0.023	0.595 $\pm$ 0.091	0.589 $\pm$ 0.060	0.251 $\pm$ 0.025	0.979 $\pm$ 0.036	0.510 $\pm$ 0.048	0.397 $\pm$ 0.046	0.281 $\pm$ 0.014
RSEC-Z [TKDD, 2019]	0.291 $\pm$ 0.027	0.535 $\pm$ 0.110	0.595 $\pm$ 0.055	0.252 $\pm$ 0.021	0.915 $\pm$ 0.063	0.542 $\pm$ 0.034	0.365 $\pm$ 0.050	0.270 $\pm$ 0.010
DREC [Neurocomputing, 2019]	0.326 $\pm$ 0.024	0.776 $\pm$ 0.048	0.628 $\pm$ 0.007	0.252 $\pm$ 0.011	0.922 $\pm$ 0.057	0.731 $\pm$ 0.037	0.404 $\pm$ 0.034	0.268 $\pm$ 0.013
SPCE [TNLNS, 2021]	0.429 $\pm$ 0.072	0.811 $\pm$ 0.039	0.596 $\pm$ 0.082	0.243 $\pm$ 0.036	0.973 $\pm$ 0.041	0.627 $\pm$ 0.062	0.401 $\pm$ 0.032	0.323 $\pm$ 0.052
ECPCS-MC [TSMC-S, 2021]	0.343 $\pm$ 0.020	0.621 $\pm$ 0.034	0.631 $\pm$ 0.031	0.249 $\pm$ 0.010	0.942 $\pm$ 0.055	0.649 $\pm$ 0.031	0.366 $\pm$ 0.029	0.277 $\pm$ 0.006
ECPCS-HC [TSMC-S, 2021]	0.462 $\pm$ 0.021	0.809 $\pm$ 0.015	0.669 $\pm$ 0.060	0.283 $\pm$ 0.024	0.985 $\pm$ 0.027	0.668 $\pm$ 0.046	0.361 $\pm$ 0.034	0.279 $\pm$ 0.009
TRCE [AAAI, 2021]	0.311 $\pm$ 0.027	0.740 $\pm$ 0.100	0.673 $\pm$ 0.029	0.245 $\pm$ 0.014	0.958 $\pm$ 0.067	0.659 $\pm$ 0.042	0.363 $\pm$ 0.040	0.280 $\pm$ 0.021
LWEA [TCYB, 2018]	0.441 $\pm$ 0.032	0.544 $\pm$ 0.026	0.649 $\pm$ 0.048	0.260 $\pm$ 0.016	0.941 $\pm$ 0.079	0.733 $\pm$ 0.041	0.386 $\pm$ 0.033	0.280 $\pm$ 0.017
Proposed	<b>0.603<math>\pm</math>0.057</b>	<b>0.823<math>\pm</math>0.012</b>	<b>0.729<math>\pm</math>0.018</b>	<b>0.322<math>\pm</math>0.019</b>	<b>0.991<math>\pm</math>0.003</b>	<b>0.750<math>\pm</math>0.046</b>	<b>0.411<math>\pm</math>0.048</b>	<b>0.368<math>\pm</math>0.020</b>

Fig. 2 visually compares the LWCA matrix, the CA matrix of our method, their difference and the ground truth one on the Aggregation dataset. We can see that the proposed method can considerably build more strong and reliable links than LWCA, which is much closer to the ideal one. Moreover, it can also weaken the wrong entries of the LWCA matrix (please zoom in the highlighted regions in Fig. 2(c)). This further explains why our method can significantly improve the clustering performance compared with LWEA.

### C. Adaptation to Diverse CAs

In this subsection, we check whether the proposed approach can adapt to other CA matrices beside LWCA. Here we used the CA matrix from EAC [9] and the similarity matrix PTS from PTA [13] as the input, and assessed the performance of our method on them, respectively. The associated results are listed in Tables V and VI, where the proposed model consistently promotes the clustering performances of original algorithms to a great extent on all eight datasets w.r.t. all three metrics. To be specific, when compared with EAC, the average improvements of our method are around 30% w.r.t. ARI, 15% w.r.t. NMI and 20% w.r.t. F-score. Especially, our method has pushed these three metrics nearly up to 1 on the Aggregation dataset. The improvements on PTA are 35%, 15%, 30% on average, and 120%, 25%, 75% singly on the Ecoli dataset w.r.t. ARI, NMI and F-score, which is remarkable. Note that after the self-enhancement procedure by our method, when referring to Tables II, III, IV, EAC and PTA-AL will attain the highest ARI/NMI/F-score on 6/5/7 and 6/3/6 datasets over all the compared state-of-the-art algorithms respectively, while these numbers are only 0/0/0 and 1/0/1 corresponding to their original algorithms. Therefore, we can conclude that the proposed method can enhance diverse CA matrices significantly, illustrating its robustness.

### D. Influence of Ensemble Size

Fig. 5 evaluates the clustering performance w.r.t. ARI of the proposed method and all the compared methods with

TABLE V  
ILLUSTRATION OF THE CLUSTERING IMPROVEMENT ON EAC W.R.T. ARI, NMI AND F-SCORE.

Metric	ARI		NMI		F-score	
	Method	EAC	Proposed	EAC	Proposed	EAC
Caltech20	0.313	<b>0.490</b>	0.467	<b>0.495</b>	0.386	<b>0.573</b>
Ecoli	0.548	<b>0.753</b>	0.651	<b>0.717</b>	0.649	<b>0.823</b>
LS	0.467	<b>0.638</b>	0.563	<b>0.675</b>	0.575	<b>0.714</b>
FCT	0.121	<b>0.146</b>	0.210	<b>0.241</b>	0.268	<b>0.305</b>
Aggregation	0.896	<b>0.989</b>	0.942	<b>0.984</b>	0.916	<b>0.991</b>
Texture	0.575	<b>0.673</b>	0.713	<b>0.802</b>	0.617	<b>0.707</b>
UMIST	0.333	<b>0.368</b>	0.651	<b>0.690</b>	0.372	<b>0.407</b>
SPF	0.057	<b>0.086</b>	0.123	<b>0.191</b>	0.271	<b>0.358</b>

TABLE VI  
ILLUSTRATION OF THE CLUSTERING IMPROVEMENT ON PTA-AL W.R.T. ARI, NMI AND F-SCORE.

Metric	ARI		NMI		F-score	
	Method	PTA	Proposed	PTA	Proposed	PTA
Caltech20	0.356	<b>0.439</b>	0.440	<b>0.475</b>	0.436	<b>0.537</b>
Ecoli	0.340	<b>0.738</b>	0.561	<b>0.700</b>	0.460	<b>0.811</b>
LS	0.593	<b>0.664</b>	0.635	<b>0.687</b>	0.673	<b>0.735</b>
FCT	0.136	<b>0.190</b>	0.242	<b>0.277</b>	0.271	<b>0.335</b>
Aggregation	0.600	<b>0.896</b>	0.786	<b>0.932</b>	0.681	<b>0.920</b>
Texture	0.658	<b>0.702</b>	0.772	<b>0.800</b>	0.691	<b>0.730</b>
UMIST	0.323	<b>0.370</b>	0.633	<b>0.687</b>	0.361	<b>0.411</b>
SPF	0.081	<b>0.098</b>	0.152	<b>0.188</b>	0.261	<b>0.337</b>

different numbers of base clusterings as input. From Fig. 5 we can observe that with a bigger ensemble size, most methods generally perform better, which is consistent with the basic idea of ensemble clustering that combining a set of clustering results can generate a better one. It is noticeable that on 5 out of 8 datasets, our method keeps a strictly monotonic increasing ARI when the ensemble size increases. In contrast, some of the compared methods sometimes experience an opposite trend such as DREC and TRCE. Moreover, it is evident that the proposed method outperforms all the compared methods with different ensemble sizes except case  $m = 10$  on Ecoli, being the most robust model among all comparisons. On datasets Caltech20, LS and FCT, the performance of our method is far

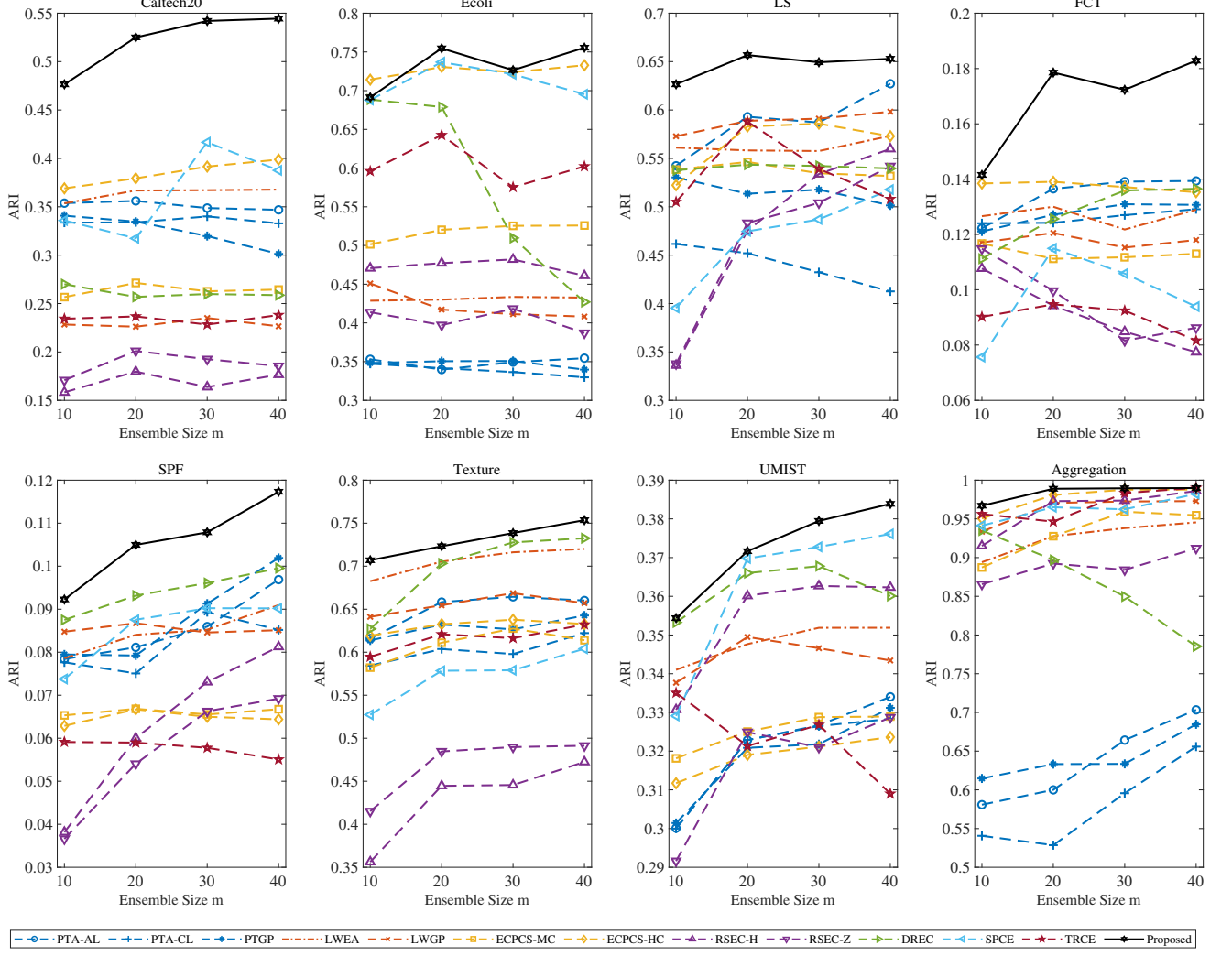


Fig. 5. Clustering performances of different algorithms by varying ensemble size w.r.t. ARI.

TABLE VII  
EXECUTION TIME OF ALGORITHMS INVOLVING AN ITERATION PROCESS  
ON ALL DATASETS. WE HIGHLIGHT THE FASTEST AND THE SECOND  
FASTEST ONES BY BOLD AND UNDERLINE.

Time(s)	RSEC-H	RSEC-Z	DREC	SPCE	TRCE	Proposed
Caltech20	700	707	<b>2.16</b>	39.4	31.5	<u>19.5</u>
Ecoli	2.91	2.94	<u>0.130</u>	0.273	0.491	<b>0.0862</b>
LS	14006	14107	<b>21.2</b>	1068	354	<u>277</u>
FCT	3633	3663	<b>4.24</b>	244	131	<u>60.3</u>
Aggregation	17.0	17.1	<b>0.167</b>	2.53	2.22	<u>1.17</u>
Texture	8207	8271	<b>6.14</b>	409	262	<u>164</u>
UMIST	8.41	8.48	<u>0.309</u>	2.50	2.79	<b>0.292</b>
SPF	285	288	<b>0.250</b>	39.5	17.1	<u>12.5</u>

ahead of compared methods, and even produce better with 10 input base clusterings than all the compared methods though they take 40 base clusterings as input.

### E. Ablation Study

In this section, we study the necessity of the involved two terms in our method. First, we dropped the Laplacian regu-

larization term, then the proposed model is degenerated into Eq. (3), and we named this case as “w/o  $\text{tr}(\mathbf{C}^\top \Phi \mathbf{C})$ ”. Second, we removed the matrix-completion constraint  $\Psi_\Omega(\mathbf{E}) = \mathbf{0}$ , naming it as “w/o  $\Psi_\Omega(\mathbf{E}) = \mathbf{0}$ ”.

The clustering performance without those terms are shown in Table VIII. It is obvious that “w/o  $\text{tr}(\mathbf{C}^\top \Phi \mathbf{C})$ ” always receives the worst scores, indicating that Laplacian regularization plays a leading role in propagating high-confidence information. Additionally, the average performance of “w/o  $\Psi_\Omega(\mathbf{E}) = \mathbf{0}$ ” exceeds that of the proposed method slightly on Texture and UMIST, while falls behind it on the other six datasets distinctly. Thus, it can be concluded that retaining those crucial HC values also contributes to enhancing the co-association matrix.

### F. Execution Time

In Table VII, we count the average running time of our method with five compared methods that also involve an iteration optimization process, i.e., RSEC-H, RSEC-Z, DREC, SPCE and TRCE, on all the datasets. Table VII suggests that the proposed method is more efficient than RSEC-H, RSEC-Z,

TABLE VIII  
ABLATION STUDY ON THE PROPOSED METHOD W.R.T. ARI, NMI AND F-SCORE.

Metric	Algorithm	Caltech20	Ecoli	LS	FCT	Aggregation	Texture	UMIST	SPF
ARI	w/o $\text{tr}(\mathbf{C}^\top \Phi \mathbf{C})$	0.367	0.430	0.558	0.130	0.928	0.705	0.348	0.084
	w/o $\Psi_\Omega(\mathbf{E}) = \mathbf{0}$	0.515	0.699	0.646	0.174	0.976	<b>0.732</b>	<b>0.373</b>	0.102
	Proposed	<b>0.525</b>	<b>0.754</b>	<b>0.657</b>	<b>0.179</b>	<b>0.989</b>	0.723	0.371	<b>0.105</b>
NMI	w/o $\text{tr}(\mathbf{C}^\top \Phi \mathbf{C})$	0.480	0.615	0.630	0.236	0.958	0.794	0.664	0.156
	w/o $\Psi_\Omega(\mathbf{E}) = \mathbf{0}$	<b>0.497</b>	0.690	0.677	0.273	0.978	<b>0.813</b>	0.685	0.197
	Proposed	<b>0.497</b>	<b>0.716</b>	<b>0.685</b>	<b>0.276</b>	<b>0.984</b>	0.811	<b>0.692</b>	<b>0.198</b>
F-score	w/o $\text{tr}(\mathbf{C}^\top \Phi \mathbf{C})$	0.441	0.544	0.649	0.260	0.941	0.733	0.386	0.280
	w/o $\Psi_\Omega(\mathbf{E}) = \mathbf{0}$	0.587	0.786	0.720	0.311	0.981	<b>0.757</b>	<b>0.413</b>	0.344
	Proposed	<b>0.603</b>	<b>0.823</b>	<b>0.729</b>	<b>0.322</b>	<b>0.991</b>	0.750	0.411	<b>0.348</b>

SPCE and TRCE due to the convexity of the proposed model and the low computational complexity of the proposed optimization algorithm. Besides, our method is more time-saving than DREC on the Ecoli and UMIST datasets, but runs slower than DREC when the scale of dataset gets larger, mainly because DREC uses the microcluster-based representation that reduces the scale of the problem. Considering that our method significantly outperforms DREC in clustering performance, a little sacrifice in running time is acceptable.

## V. CONCLUSION

In this paper, we have presented a novel CA-matrix self-enhancement model for ensemble clustering. Without any extra information, our method can promote a CA matrix by exploiting the highly-reliable information and denoising error connections simultaneously. We formulated this model as a well-defined convex optimization problem and proposed an ADMM-based algorithm to solve it with convergence and global optimum theoretically guaranteed. Extensive experimental comparisons validate that the proposed model outperforms the state-of-the-art methods significantly in clustering performance. Moreover, it is robust to hyper-parameters, can adapt to diverse CA matrices, produces better performance with more base clusterings, and is more efficient than many other approaches.

## REFERENCES

- [1] J. A. Hartigan and M. A. Wong, “Algorithm as 136: A k-means clustering algorithm,” *Journal of the royal statistical society. series c (applied statistics)*, vol. 28, no. 1, pp. 100–108, 1979.
- [2] A. K. Jain, M. N. Murty, and P. J. Flynn, “Data clustering: a review,” *ACM computing surveys (CSUR)*, vol. 31, no. 3, pp. 264–323, 1999.
- [3] Y. Cheng, “Mean shift, mode seeking, and clustering,” *IEEE transactions on pattern analysis and machine intelligence*, vol. 17, no. 8, pp. 790–799, 1995.
- [4] C. M. Bishop, “Pattern recognition,” *Machine learning*, vol. 128, no. 9, 2006.
- [5] U. Von Luxburg, “A tutorial on spectral clustering,” *Statistics and computing*, vol. 17, no. 4, pp. 395–416, 2007.
- [6] J. Xie, R. Girshick, and A. Farhadi, “Unsupervised deep embedding for clustering analysis,” in *International conference on machine learning*. PMLR, 2016, pp. 478–487.
- [7] A. Strehl and J. Ghosh, “Cluster ensembles—a knowledge reuse framework for combining multiple partitions,” *Journal of machine learning research*, vol. 3, no. Dec, pp. 583–617, 2002.
- [8] D. Huang, C.-D. Wang, and J.-H. Lai, “Locally weighted ensemble clustering,” *IEEE Transactions on Cybernetics*, vol. 48, no. 5, pp. 1460–1473, 2018.
- [9] A. L. Fred and A. K. Jain, “Combining multiple clusterings using evidence accumulation,” *IEEE transactions on pattern analysis and machine intelligence*, vol. 27, no. 6, pp. 835–850, 2005.
- [10] X. Z. Fern and C. E. Brodley, “Solving cluster ensemble problems by bipartite graph partitioning,” in *Proceedings of the twenty-first international conference on Machine learning*, 2004, p. 36.
- [11] Z. Li, X.-M. Wu, and S.-F. Chang, “Segmentation using superpixels: A bipartite graph partitioning approach,” in *2012 IEEE conference on computer vision and pattern recognition*. IEEE, 2012, pp. 789–796.
- [12] T. Li and C. Ding, “Weighted consensus clustering,” in *Proceedings of the 2008 SIAM International Conference on Data Mining*. SIAM, 2008, pp. 798–809.
- [13] D. Huang, J.-H. Lai, and C.-D. Wang, “Robust ensemble clustering using probability trajectories,” *IEEE Transactions on Knowledge and Data Engineering*, vol. 28, no. 5, pp. 1312–1326, 2016.
- [14] P. Zhou, L. Du, X. Liu, Y.-D. Shen, M. Fan, and X. Li, “Self-paced clustering ensemble,” *IEEE Transactions on Neural Networks and Learning Systems*, vol. 32, no. 4, pp. 1497–1511, 2021.
- [15] K. Fan, “On a theorem of weyl concerning eigenvalues of linear transformations i,” *Proceedings of the National Academy of Sciences of the United States of America*, vol. 35, no. 11, p. 652, 1949.
- [16] P. Zhou, L. Du, and X. Li, “Self-paced consensus clustering with bipartite graph,” in *Proceedings of the Twenty-Ninth International Conference on International Joint Conferences on Artificial Intelligence*, 2021, pp. 2133–2139.
- [17] P. Zhou, L. Du, Y.-D. Shen, and X. Li, “Tri-level robust clustering ensemble with multiple graph learning,” in *Proceedings of the AAAI Conference on Artificial Intelligence*, vol. 35, 2021, pp. 11125–11133.
- [18] J. Yi, T. Yang, R. Jin, A. K. Jain, and M. Mahdavi, “Robust ensemble clustering by matrix completion,” in *2012 IEEE 12th international conference on data mining*. IEEE, 2012, pp. 1176–1181.
- [19] P. Zhou, L. Du, H. Wang, L. Shi, and Y.-D. Shen, “Learning a robust consensus matrix for clustering ensemble via kullback-leibler divergence minimization,” in *Twenty-Fourth International Joint Conference on Artificial Intelligence*, 2015.
- [20] Z. Tao, H. Liu, S. Li, Z. Ding, and Y. Fu, “Robust spectral ensemble clustering via rank minimization,” *ACM Transactions on Knowledge Discovery from Data (TKDD)*, vol. 13, no. 1, pp. 1–25, 2019.
- [21] Y. Jia, H. Liu, J. Hou, S. Kwong, and Q. Zhang, “Semisupervised affinity matrix learning via dual-channel information recovery,” *IEEE Transactions on Cybernetics*, 2021.
- [22] S. Boyd, N. Parikh, and E. Chu, *Distributed optimization and statistical learning via the alternating direction method of multipliers*. Now Publishers Inc, 2011.
- [23] L. Fei-Fei, R. Fergus, and P. Perona, “Learning generative visual models from few training examples: An incremental bayesian approach tested on 101 object categories,” in *2004 conference on computer vision and pattern recognition workshop*. IEEE, 2004, pp. 178–178.
- [24] H. Wechsler, J. P. Phillips, V. Bruce, F. F. Soulie, and T. S. Huang, *Face recognition: From theory to applications*. Springer Science & Business Media, 2012, vol. 163.
- [25] J. Alman and V. V. Williams, “A refined laser method and faster matrix multiplication,” in *Proceedings of the 2021 ACM-SIAM Symposium on Discrete Algorithms (SODA)*. SIAM, 2021, pp. 522–539.
- [26] J. Zhou, H. Zheng, and L. Pan, “Ensemble clustering based on dense representation,” *Neurocomputing*, vol. 357, pp. 66–76, 2019.
- [27] D. Huang, C.-D. Wang, H. Peng, J. Lai, and C.-K. Kwoh, “Enhanced ensemble clustering via fast propagation of cluster-wise similarities,”

*IEEE Transactions on Systems, Man, and Cybernetics: Systems*, vol. 51, no. 1, pp. 508–520, 2021.

[28] N. X. Vinh, J. Epps, and J. Bailey, “Information theoretic measures for clusterings comparison: Variants, properties, normalization and correction for chance,” *The Journal of Machine Learning Research*, vol. 11, pp. 2837–2854, 2010.